Journal of Solid State Chemistry 219 (2014) 173–178

Contents lists available at ScienceDirect

Journal of Solid State Chemistry

journal homepage: www.elsevier.com/locate/jssc

Structural and magnetic behavior of the cubic oxyfluoride $SrFeO_2F$ studied by neutron diffraction

Corey M. Thompson [a,b,*], Colin K. Blakely [c], Roxana Flacau [d], John E. Greedan [a,b], Viktor V. Poltavets [c]

[a] Department of Chemistry, McMaster University, Hamilton, ON, Canada L8S 4M1
[b] Brockhouse Institute of Materials Research, McMaster University, Hamilton, ON, Canada L8S 4M1
[c] Department of Chemistry, Michigan State University, East Lansing, MI 48824, USA
[d] Canadian Neutron Beam Centre, National Research Council, Chalk River Laboratories, Chalk River, ON, Canada K0J 1J0

ARTICLE INFO

Article history:
Received 25 May 2014
Received in revised form
16 July 2014
Accepted 16 July 2014
Available online 24 July 2014

Keywords:
$SrFeO_2F$
Neutron diffraction
Oxyfluoride
Antiferromagnetism

ABSTRACT

The oxyfluoride $SrFeO_2F$ has been prepared via a low temperature route involving the infinite-layer $SrFeO_2$ and XeF_2. $SrFeO_2F$ crystallizes in the cubic space group *Pm*-3*m* with disordered oxygen and fluorine atoms on the anion site. Recent reports demonstrated that $SrFeO_2F$ is antiferromagnetic at room temperature and the zero field cooled and field cooled curves diverge at ~150 K and ~60 K, suggesting that the material has a spin glassy magnetic state at low temperatures. In this article, variable-temperature neutron diffraction (4–723 K) was performed to clarify the magnetic behavior observed in this material. Neutron powder diffraction measurements confirmed the antiferromagnetic (AFM) ordering of the system at room temperature. Below 710(1) K, the magnetic structure is a G-type AFM structure characterized by a propagation vector $\boldsymbol{k}=(\frac{1}{2},\frac{1}{2},\frac{1}{2})$. The ordered moments on Fe^{3+} are $4.35(6)\mu_B$ at 4 K and $4.04(5)\mu_B$ at 290 K. Our results indicate that the cubic structure is retained all the way to base temperature (4 K) in contrast to $PbFeO_2F$. These results are compared with those of Pb and Ba analogs which exhibit very similar magnetic behavior. Furthermore, the observation of magnetic reflections at 4 K in the diffraction pattern shows the absence of the previously proposed spin glassy behavior at low temperatures. Previous proposals to explain the ZFC/FC divergences are examined.

1. Introduction

Oxyfluoride materials are of great interest due to their recent technological applications such as light emitting diodes, electrolytes for fuel cells, and electrodes for aqueous batteries [1–3]. The discovery of the superconducting oxyfluoride $Sr_2CuO_2F_{2+x}$ has led to increased efforts to synthesize other oxyfluoride compounds [4–7]. In this regard many oxyfluoride phases have been prepared using a number of fluorination agents, e.g. F_2 gas, transition metal fluorides, XeF_2, and poly(vinylidene fluoride) (PDVF) [8–11]. Among these oxyfluorides a number have accumulated interest due to their unusual magnetic behavior, for instance, $PbFeO_2F$, $BaFeO_2F$, and $SrFeO_2F$ [12–19].

$PbFeO_2F$ has been synthesized at 1000 °C under high pressure (~5 GPa) [12]. This compound crystallizes in a cubic perovskite-type (*Pm*-3*m*) structure where the Pb ions are shifted from the ideal A site and in the $<110>$ directions [13]. No evidence for the ordering of O and F ions were observed therefore the ions are assumed to be randomly distributed over the anion site. $PbFeO_2F$ exhibited antiferromagnetic ordering below $T_N=655(5)$ K [14]. The magnetic structure is G-type antiferromagnetic with a propagation vector $\boldsymbol{k}=(\frac{1}{2},\frac{1}{2},\frac{1}{2})$ and Fe^{3+} moment of $3.83\mu_B$ at 298 K which increases to $4.1\mu_B$ at 3.4 K. This material shows a complex structural history. It is cubic, *Pm*-3*m*, in the as-quenched state at room temperature but transforms to a tetragonal form when heated, transforming again to cubic above ~475 K. This transformation is reversible and the room temperature form is indeed tetragonal with a complex $a\times a\times 5c$ supercell confirmed by both X-ray and electron diffraction. It is of interest to determine if such structural transformations occur for $SrFeO_2F$.

$BaFeO_2F$ has been synthesized by both the high pressure route and recently via the low temperature polymer method using PDVF [12,15,16]. Similarly to $PbFeO_2F$, $BaFeO_2F$ adopts a cubic structure (*Pm*-3*m*) with no apparent ordering of the O/F ions. However, a 0.25 Å off-site shift for Fe was proposed due to the large Ba^{2+} ion, leading to underbonding at the iron site. $BaFeO_2F$ orders antiferromagnetically below $T_N=645(5)$ K again with a G-type structure.

Recently, we and others have reported on the perovskite oxyfluoride $SrFeO_2F$. This compound has been synthesized both

* Corresponding author at: Department of Chemistry, McMaster University, Hamilton, ON, Canada L8S 4M1. Fax: +1 905 521 2773.
E-mail address: thompco@mcmaster.ca (C.M. Thompson).

http://dx.doi.org/10.1016/j.jssc.2014.07.019
0022-4596/

by the polymer method using PVDF and $SrFeO_{3-\delta}$ at 400 °C and also via reaction between the infinite layer $SrFeO_2$ and XeF_2 at 150 °C [17,18]. Both samples crystallize in the cubic *Pm*-3*m* space group with the same unit cell parameter, 3.955 Å, with no long range ordering of oxygen and fluorine atoms, suggesting that the two different synthetic methods yield the same material. If there are differences they will likely occur on the short range length scale. For example, Mössbauer spectroscopic data reported for the $SrFeO_2/XeF_2$ prepared sample indicated a preference for cis-FeO_4F_2 octahedra [18]. More recently, Clemens et al. noted that $SrFeO_2F$ can be described by an orthorhombic structure, *Imma*, instead of *Pm*-3*m* based on symmetry mode decomposition analysis [19]. However, the unit cell constants remain metrically cubic. From Mössbauer data Berry et al. report an antiferromagnetic ordering temperature of T_N=685(5) K and divergence of the zero field (ZFC) and field-cooled (FC) curves below 150 K in the magnetic susceptibility. Blakely et al. report antiferromagnetic ordering at room temperature, also from Mössbauer data, and a ZFC/FC divergence below 60 K. There have been at least two proposals to explain the ZFC/FC divergent behavior. Initially, Berry et al. suggested the existence of a "random spin" state below 300 K based in part on interpretation of Mössbauer data. A later proposal involved the onset of spin-canting, albeit at a temperature well below T_N, which is unusual [19]. Recently, Blakely et al. have shown the absence of a strong frequency shift in a.c. susceptibility data for their sample, which mitigates against a spin glassy transition [18]. These issues will be revisited.

Obviously, these reported studies leave some open questions and further examination is justified. To help unravel the mystery behind the observed structural and magnetic behavior in these materials we have carried out variable-temperature neutron diffraction measurements on a sample of $SrFeO_2F$, specifically that prepared via the reaction between the infinite layer $SrFeO_2$ and XeF_2 [18]. Our studies suggest no evidence of any structural change with increasing temperature in contrast to $PbFeO_2F$ and that the structure can be characterized by the standard cubic *Pm*-3*m* structure throughout the whole temperature range (4–723 K). There is no indication of spin randomization or spin glassy behavior as evidenced by strong magnetic reflections observed in the 4 K neutron diffraction pattern. Furthermore, we obtained a higher magnetic ordering temperature of 710(1) K rather than 685 (5) K reported earlier by Berry et al. [17]. Lastly, we conclude with a critical examination of the various explanations of the low temperature magnetic behavior observed in $SrFeO_2F$ prepared by both groups and compare $SrFeO_2F$ to the other oxyfluorides $PbFeO_2F$ and $BaFeO_2F$.

2. Experimental section

2.1. Synthesis

A ~2 g powder sample of $SrFeO_2F$ was prepared in multiple separate syntheses via the method reported earlier by Blakely et al. [18] i.e. via the reaction of infinite-layered $SrFeO_2$ and XeF_2 (15% excess). Stoichiometric amounts of both starting materials was weighed in a glove box and loaded into a Teflon sleeve. The sleeve was sealed in a steel autoclave then removed from the glove box and placed in a furnace. The mixture was heated for 48 h at 150 °C and the products were stored under nitrogen due to the moisture sensitivity of the oxyfluoride.

2.2. Neutron diffraction

Powder neutron diffraction measurements were performed on the C2 diffractometer at the Canadian Neutron Beam Centre at Chalk River, Ontario. The data were collected at 16 different temperatures from 4 K to 723 K. A wavelength of 1.33025 Å with 2θ step size of 0.100° was used to collect data within the 2θ range of 12.0–92.0°. Measurements were performed on a sample of ~2 g held in a cylindrical molybdenum (high-temperature scans; >290 K) or vanadium (low temperature scans; ≤290 K) container in a top-loading closed-cycle refrigerator. The Rietveld refinements were performed excluding peaks both from the intense scattering of the molybdenum sample can (~2 mm in wall thickness; high-temperature data) and broad impurity peaks of poorly crystallized SrF_2 which result from partial decomposition occurring during the fluorination process (low-temperature data). The crystal and magnetic structures were refined using FullProf [20].

3. Results and discussion

3.1. Crystal structure

Rietveld refinement results of the 290 K and 723 K neutron diffraction data confirmed that $SrFeO_2F$ crystallizes in the cubic perovskite structure *Pm*-3*m* depicted in Fig. 1, in accordance with previously reported results [17–19]. The lattice constants, displacement parameters, and agreement indices are provided in Table 1. Fig. 2 shows the refinement results of the neutron powder diffraction data at 290 K and 723 K. $SrFeO_2F$ is isostructural with the previously reported compounds $BaFeO_2F$ and $PbFeO_2F$ (for $T>475$ K), former having been synthesized by the low temperature polymer (PDVF) method and the latter by the high temperature and high pressure method [12–16]. The oxygen and fluorine atoms are long range disordered on the anion site and no ordering of these atoms was detected and/or could be confirmed via neutron diffraction due to the similar neutron scattering lengths of both oxygen (5.803 fm) and fluorine (5.654 fm). Refinement of the anion site led to full occupancies, therefore, both the oxygen and fluorine atoms were fixed to their respective site occupancy ratios, 2/3 and 1/3 respectively. Bond valence sum calculations were performed and are provided in Table 2, the calculations for the cations (Sr and Fe) were executed with the expected coordinated ratios of oxygen and fluorine (2/3O and 1/3F) [21,22]. The bond valence for iron is +2.97 at 723 K and +3.10 at 290 K which confirms that the oxidation state for iron is +3. The bond valence for strontium, oxygen, and fluorine at 723 K are +1.66, −1.67, −1.32, respectively, and are consistent with those reported for $PbFeO_2F$ [13].

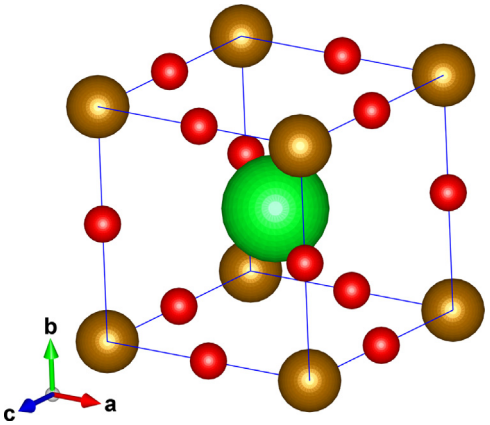

Fig. 1. Crystal structure of $SrFeO_2F$. Strontium, iron, and oxygen/fluorine atoms are shown in green, gold, and red spheres, respectively. (For interpretation of the references to color in this figure legend, the reader is referred to the web version of this article.)

Neutron diffraction data were also collected at 4 K. The lattice constants, atomic displacement parameters, and agreement indices are provided in Table 3 and the refinement results are shown in Fig. 2. The refinement results indicate that the crystal lattice preserves cubic symmetry at 4 K with a_0=3.9438(5) Å.

3.2. Magnetic structure

Previous magnetic susceptibility and Mössbauer spectroscopy measurements indicated antiferromagnetism in $SrFeO_2F$ at room temperature [17]. In order to determine the actual magnetic structure neutron powder diffraction patterns were recorded at various temperatures from 723 K to 4 K. The diffraction pattern collected at 723 K confirms the cubic *Pm*-3*m* structure, while for lower temperatures additional reflections are expected due to the antiferromagnetic alignment of the iron moments. Indeed, this is the case, as Fig. 3 shows the 723 K and 373 K neutron diffraction patterns along with the difference intensity. The new peaks can be indexed with a propagation vector $\boldsymbol{k}=(\frac{1}{2},\frac{1}{2},\frac{1}{2})$, indicating a G-type antiferromagnetic structure where all the adjacent Fe^{3+} ions are antiferromagnetically coupled (Fig. 4).

Table 1
Neutron diffraction refinement results of $SrFeO_2F$ at 290 K. The results for the 723 K data are reported in [] below the 290 K data.

	x	*y*	*z*	B_{iso} (Å^2)
Sr	0.5	0.5	0.5	0.6(1) [1.9(3)]
Fe	0	0	0	1.6(1) [2.7(3)]
O/F	0	0	0.5	2.0(1) [3.3(3)]
a_0 (Å)	3.9529(5) [3.984(1)]			
Fe^{3+} (μ_B)	4.04(5)			
χ^2	4.01 [3.78]		R_{Bragg}	9.54 [28.4]
R_p	3.53 [7.02]		R_F	5.71 [18.8]
R_{wp}	4.73 [9.18]		R_{Mag}	23.5
R_{exp}	2.36 [4.72]			

Fig. 5 shows the temperature dependence of the refined iron moments from 4 K to 723 K. The Fe^{3+} moments are 4.35(6)μ_B and 4.04(5)μ_B at 4 K and 290 K, respectively. These moments are typical for an S=5/2 ion, which are between 4.0 and 4.5μ_B for many Fe^{3+} oxides. From Fig. 5 the antiferromagnetic ordering temperature, T_N, is somewhere between 698 K and 723 K. T_N can be determined by tracking the intensity of the most intense magnetic reflection, for instance, the $(\frac{1}{2},\frac{1}{2},\frac{1}{2})$ magnetic peak. The intensity of the magnetic peaks is proportional to the moment squared ($M_{Fe}{}^2$), therefore, the square root of the intensity ($I^{1/2}$) is plotted versus temperature. T_N can be estimated by fitting the data near T_N to the function $I^{1/2}=A\times((T_N-T)/T_N)^{\beta}$, where β is a "critical

Table 2
Selected bond distances and calculated bond valence sums in $SrFeO_2F$ at various temperatures.

	4 K	290 K	723 K
Bond distances (Å)			
Sr–O/F	2.7887(2)	2.7951(2)	2.8173(7)
Fe–O/F	1.9719(2)	1.9764(2)	1.9921(7)
Bond valence sums (BVS)[a]			
Sr	1.79[b]	1.76[b]	1.66[b]
Fe	3.13[c]	3.10[c]	2.97[c]
O	−1.78	−1.75	−1.67
F	−1.41	−1.39	−1.32

[a] Bond valence parameters used were obtained from Refs. [21,22].
[b] Used (2/3 × Sr–O)+(1/3 × Sr–F)=2.085.
[c] Used (2/3 × Fe–O)+(1/3 × Fe–F)=1.732.

Table 3
Neutron diffraction refinement results of $SrFeO_2F$ at 4 K.

	x	*y*	*z*	B_{iso} (Å^2)
Sr	0.5	0.5	0.5	0.2(1)
Fe	0	0	0	1.2(1)
O/F	0	0	0.5	1.7(1)
a_0 (Å)	3.9438(5)			
Fe^{3+} (μ_B)	4.35(6)			
χ^2	5.36		R_{Bragg}	10.7
R_p	4.05		R_F	6.72
R_{wp}	5.53		R_{Mag}	23.3
R_{exp}	2.39			

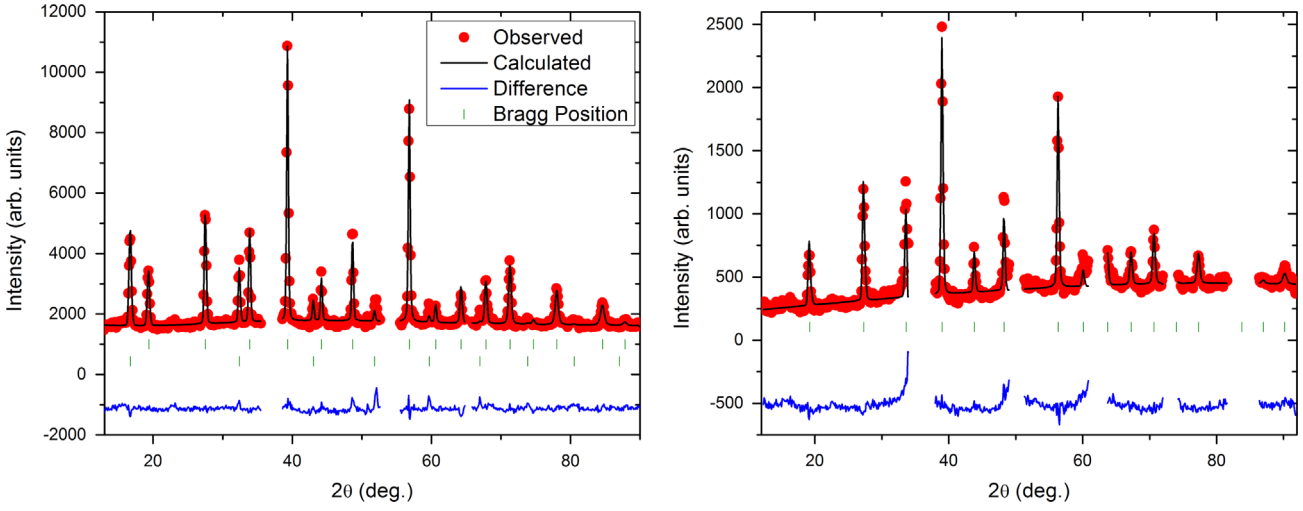

Fig. 2. Rietveld refinement of the neutron diffraction pattern at 290 K (left) and 723 K (right). The green tick marks indicate the nuclear and magnetic Bragg peaks with propagation vector $\boldsymbol{k}=(\frac{1}{2},\frac{1}{2},\frac{1}{2})$, respectively. The omitted regions correspond to broad impurity peaks of SrF_2 (290 K) or strong Bragg peaks from the Mo sample can (723 K). (For interpretation of the references to color in this figure legend, the reader is referred to the web version of this article.)

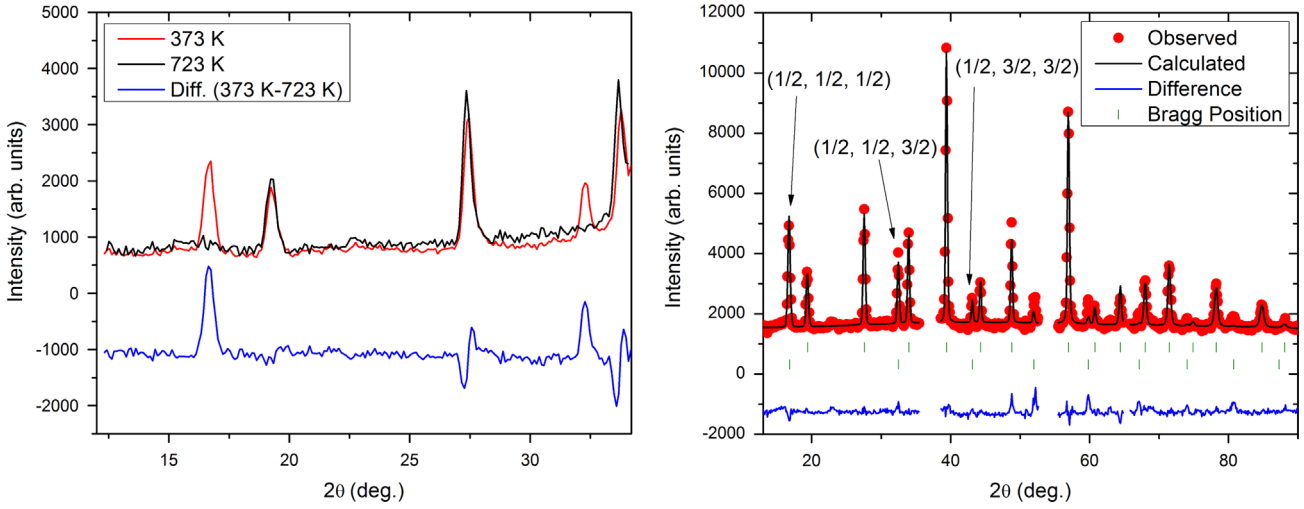

Fig. 3. Neutron diffraction patterns at 373 K and 723 K, along with the difference between the two curves (left). Refinement of the neutron diffraction pattern at 4 K (right) with propagation vector $\boldsymbol{k}=(\frac{1}{2},\frac{1}{2},\frac{1}{2})$. The green tick marks indicate the nuclear and magnetic cells, respectively. The black arrows indicate selected indexed magnetic reflections. (For interpretation of the references to color in this figure legend, the reader is referred to the web version of this article.)

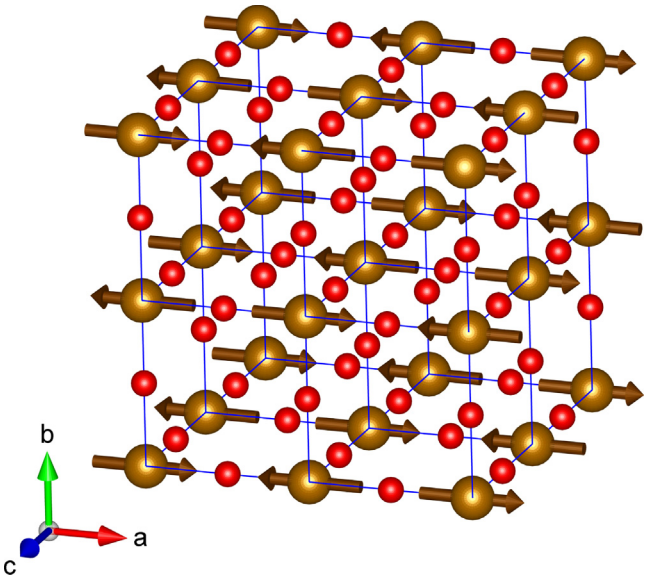

Fig. 4. The magnetic unit cell of $SrFeO_2F$. Iron and oxygen/fluorine atoms are shown in gold and red spheres, respectively. Strontium atoms are omitted for clarity and the gold arrows represent the Fe^{3+} magnetic moments in the G-type AFM structure. The moment direction is arbitrary as this cannot be determined from powder data on a cubic material. (For interpretation of the references to color in this figure legend, the reader is referred to the web version of this article.)

exponent" which can be taken as 0.36, the value appropriate for Heisenberg spins, which is the most likely case for Fe^{3+} which has no orbital magnetic moment (Fig. 6) [23]. This function describes the T-dependence of the magnetic moment as T_N is approached from lower temperatures for T near T_N. The magnetic ordering temperature T_N estimated in this manner is 710(1) K (Fig. 6).

3.3. Comparisons with previous works

As stated above, neutron diffraction experiments demonstrated that $SrFeO_2F$ retains cubic symmetry throughout the temperature range from 4 K to 723 K, in contrast to $PbFeO_2F$, which exhibited a structural change from tetragonal t-$PbFeO_2F$ to cubic c-$PbFeO_2F$ symmetry at ~470 K [14]. In addition, our results indicate that the magnetic ordering temperature is 710(1) K, which is significantly higher than that reported by Berry et al., 685(5) K, determined from Mössbauer spectroscopy measurements [17]. The disparity in ordering temperatures might be due to a difference in sample preparation methods. Our samples were prepared by a reaction between the infinite layered $SrFeO_2$ and XeF_2 at 150 °C, whereas the sample of Berry et al. was prepared using $SrFeO_{3-\delta}$ and PVDF at 400 °C [17,18].

As mentioned in Section 1, previous reports suggested that $SrFeO_2F$, while antiferromagnetically ordered at room temperature, undergoes spin randomization at lower temperatures [17]. In spin glasses, there is no long range magnetic order and the spins are randomly oriented in space and frozen in time, therefore, their neutron powder diffraction patterns will not give rise to sharp magnetic reflections. All neutron diffraction data presented here from 4 K to 698 K show sharp magnetic Bragg reflections consistent with a G-type antiferromagnetic structure with a propagation vector $\boldsymbol{k}=(\frac{1}{2},\frac{1}{2},\frac{1}{2})$. Parallel results were reported at 4 K for $BaFeO_2F$ and $PbFeO_2F$ [14–16]. Thus, there is no evidence for a transition to a spin glassy state below ~300 K in $SrFeO_2F$ as suggested by Berry et al. [17].

Both samples of $SrFeO_2F$, Berry et al. and Blakely et al., show divergences of the zero-field cooled (ZFC) and field cooled (FC) bulk susceptibility at ~150 K and ~50 K, respectively [17,18]. While random bulk spin freezing can be ruled out by the neutron diffraction data, a weak spin canting model has been proposed, similar to that for the case of $BaFeO_2F$ [16,19]. One problem with this explanation is that the most likely mechanism enabling spin canting, the Dzialoshinski–Moriya (D–M) interaction, is not allowed by symmetry for the Pm-3m perovskite structure – there exists an inversion center between nearest neighbor Fe^{3+} ions [24]. It is of course possible that a weak structural phase transition occurs upon cooling to a symmetry for which the D–M is allowed. However, it would be necessary for this to happen at different temperatures for the two different $SrFeO_2F$ samples. On the subject of different crystal symmetries, as mentioned in the Introduction, it has been proposed that *Imma* is the true space group for $SrFeO_2F$ [19]. For this space group and the Fe^{3+} ion position at 4*b*, D–M is allowed. Nonetheless, as mentioned earlier, the evidence for this symmetry is not strongly supported by the diffraction data as the unit cell is metrically cubic. In order to check if our neutron data can be described by the *Imma* structure type instead of Pm-3m, we performed a refinement on the neutron diffraction pattern recorded at 723 K, above the ordering temperature where the additional magnetic reflections are absent. This refinement did not converge indicating that, within the resolution

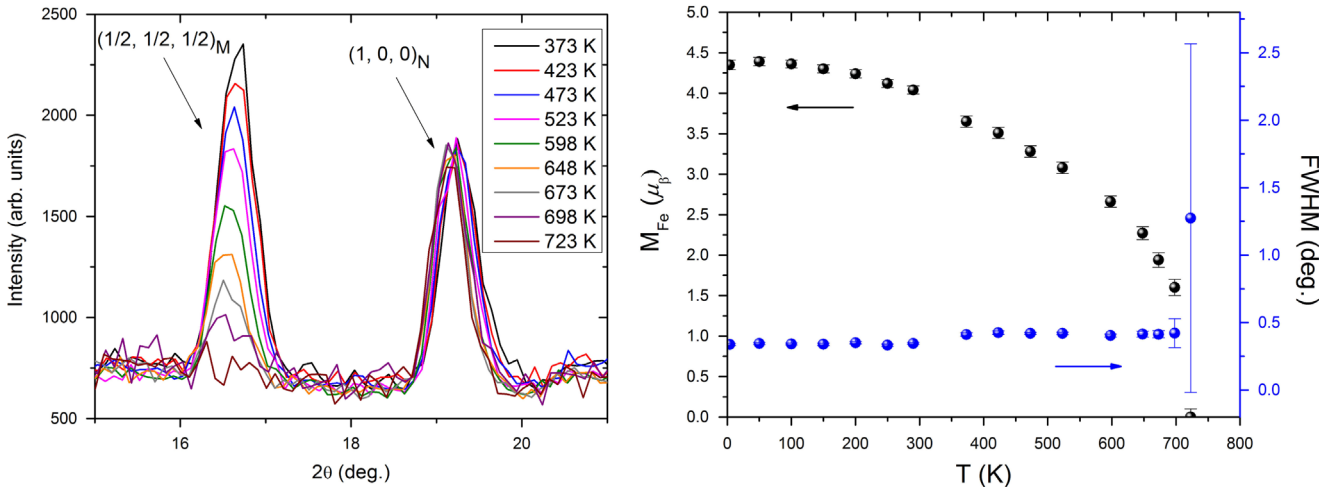

Fig. 5. Neutron diffraction patterns at 373–723 K (left) and temperature dependence of the refined Fe^{3+} magnetic moment and FWHM for the $(\frac{1}{2}, \frac{1}{2}, \frac{1}{2})$ magnetic reflection (right).

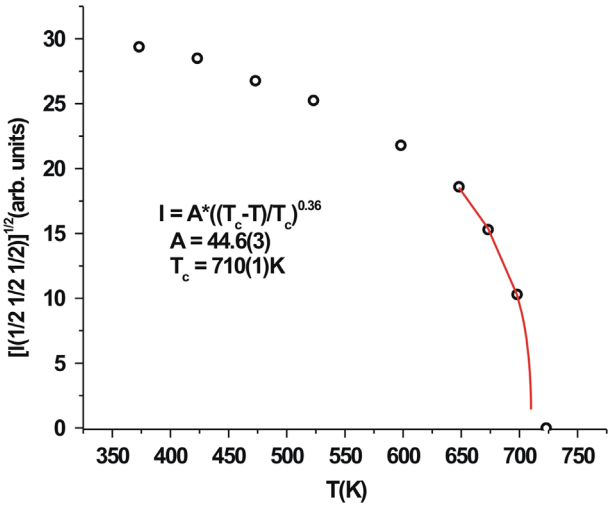

Fig. 6. Temperature dependence of the [intensity]$^{1/2}$ for the $(\frac{1}{2}, \frac{1}{2}, \frac{1}{2})$ magnetic peak. The red line is a fit of the data for $T > 648$ K to the function described above giving $T_N = 710(1)$ K. (For interpretation of the references to color in this figure legend, the reader is referred to the web version of this article.)

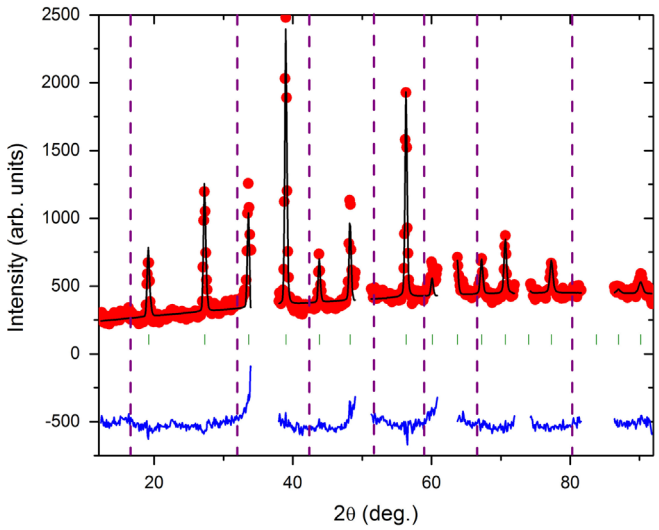

Fig. 7. Refinement of the neutron diffraction pattern at 723 K. The purple dash lines indicate the expected additional peaks of an *Imma* structure-type that are not present. (For interpretation of the references to color in this figure legend, the reader is referred to the web version of this article.)

of our neutron diffraction data, there is no evidence for *Imma* rather than *Pm*-3*m*. Fig. 7 demonstrates the refinement of the neutron data at 723 K with the cubic structure *Pm*-3*m* and includes the expected additional peak positions that would be present if the structure were *Imma*.

While the structural transition/spin canting explanation cannot be ruled out conclusively, given the above difficulties, are there mechanisms apart from spin canting which can give rise to the observed ZFC/FC divergences? While it seems clear that the vast majority of the sample volume is well described by a robust G-type antiferromagnetic order below 710 K, the contributions of relatively small sample volume components, if they are somehow decoupled from the bulk, could dominate the bulk susceptibility data at low temperatures, as at temperatures well below T_N, the majority volume spins will make little contribution. At this stage the a.c. susceptibility data of Blakely et al. can be revisited [18]. While it is true that the overall change in T_{max} with increasing frequency is very small, there is indeed a discernible shift between the range $\omega = 500$–1000 Hz and $\omega = 5000$–10,000 Hz. Oddly, the shift does not appear to be continuous with frequency but occurs as a jump between 1000 Hz ($T_{max} = 64.3$ K) and 5000 Hz ($T_{max} = 66.0$ K). From these results a shift ratio $\Delta T_{max}/T_{max}(\Delta \log \omega) \sim 0.007$ can be obtained [25]. This value is at the low end of the range reported for spin glasses. Small volume regions of the sample with such properties could arise due to short range O/F site ordering. As mentioned earlier, there is Mössbauer evidence for such ordering for samples prepared by the $SrFeO_2/XeF_2$ method [18]. As the degree and details of the short range O/F ordering would likely vary with sample preparation method, the observed differences in the ZFC/FC divergence temperatures could be understood, at least, qualitatively.

Finally, the observed results of $SrFeO_2F$ can be compared to the other aforementioned isostructural oxyfluorides, $PbFeO_2F$ and $BaFeO_2F$. Fig. 8 shows the comparison between $MFeO_2F$ (M=Sr, Pb, Ba) phases. Note that, as the cation ionic radius decreases, there is a direct correlation between the magnetic ordering temperature and the Fe–O/F distance. i.e., as the Fe–O/F distances become longer, the magnetic interaction between Fe–O/F–Fe decreases resulting in a lower magnetic ordering temperature. Surprisingly, there is a drastic change from Pb^{2+} to Sr^{2+} ions. Although there is a relatively small difference in ionic radii ($\Delta IR = 0.05$ Å) and distance between Fe–O/F ($\Delta d_{Fe-O/F} = 0.03$ Å), the change in the magnetic ordering temperature ($\Delta T_N = 55$ K) is quite large in contrast to that from Ba^{2+} to Pb^{2+} ions with $\Delta T_N = 10$ K, $\Delta IR = 0.12$ Å, and $\Delta d_{Fe-O/F} = 0.03$ Å.

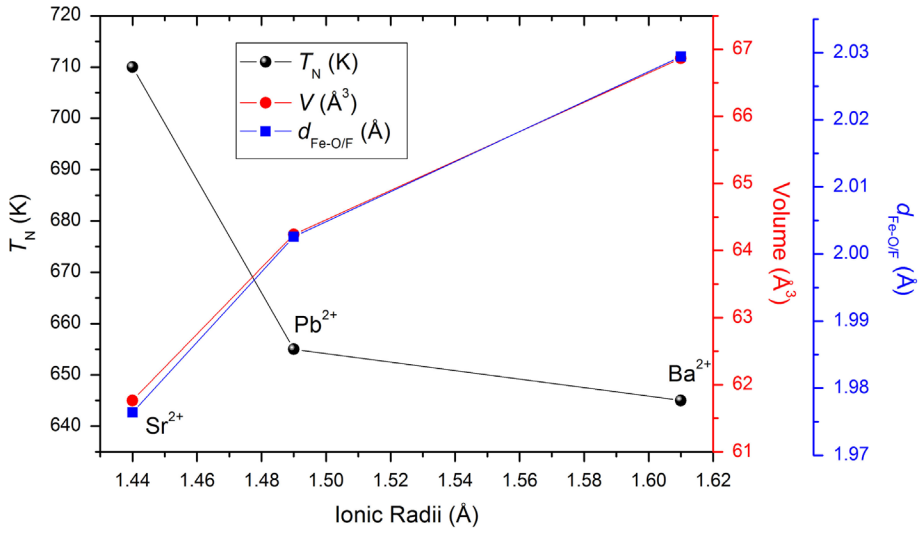

Fig. 8. Comparison between $MFeO_2F$ (M=Sr, Pb, Ba). The antiferromagnetic ordering temperature T_N, volume of the crystal lattice, and distance between Fe–O/F are shown in black, red, and blue symbols/curves, respectively. Strontium data is taken from this work. Volume and distance between Fe–O/F data was taken from room temperature results [14,15]. Lines are guides for the eye. (For interpretation of the references to color in this figure legend, the reader is referred to the web version of this article.)

4. Conclusion

Variable temperature neutron diffraction data show that $SrFeO_2F$ has antiferromagnetic order with the Type G structure over the range 4–710 K. The refined iron magnetic moment is 4.35(6)μ_B and 4.04(5)μ_B at 4 K and 290 K, respectively, establishing that Fe is indeed 3+ and is supported by BVS calculations. The cubic *Pm*-3*m* structure is maintained over the entire temperature range studied, 4–723 K, in contrast to $PbFeO_2F$ which exhibits a structural change from tetragonal to cubic at ~475 K. The Neel temperature T_N=710 (1) K is significantly higher than that from a previous report, 685(5) K obtained from Mossbauer spectroscopy, and this may be due to the difference in synthetic preparations. A previous explanation for the ZFC/FC divergence in the bulk susceptibility in terms of a spin randomization at low temperatures can be ruled out. A proposed spin canting mechanism is evaluated critically and an alternative mechanism involving small volume, bulk decoupled, spin glassy domains or clusters is proposed. Compared to Pb and Ba analogs, $SrFeO_2F$ has the highest antiferromagnetic ordering temperature which can be rationalized by a shorter Fe–O/F distance, resulting in a stronger magnetic interaction.

Acknowledgments

J.E.G. acknowledges the support of the Natural Sciences and Engineering Research Council of Canada (NSERC) in the form of a Discovery Grant. C.K.B. and V.V.P. were supported by the National Science Foundation through Grant DMR-1206718.

References

[1] C. Zhu, J. Wang, M. Zhang, X. Ren, J. Shen, Y. Yue, J. Am. Ceram. Soc. 97 (2014) 854–861.
[2] E. Sullivan, T. Vogt, ECS J. Solid State Sci. Technol. 2 (2013) R3088–R3099.
[3] G.G. Amatucci, N. Pereira, J. Fluor. Chem. 128 (2007) 243–262 (and references therein).
[4] M. Al-Mamouri, P.P. Edwards, C. Greaves, M. Slaski, Nature 369 (1994) 382–384.
[5] P.R. Slater, P.P. Edwards, C. Greaves, I. Gameson, M.G. Francesconi, J.P. Hodges, M. Al-Mamouri, M. Slaski, Physica C 241 (1995) 151–157.
[6] M. Al-Mamouri, P.P. Edwards, C. Greaves, P.R. Slater, M. Slaski, J. Mater. Chem. 5 (1995) 913–916.
[7] X. Chen, J. Liang, W. Tang, C. Wang, G. Rao, Phys. Rev. B 52 (1995) 16233–16236.
[8] C. Greaves, M.G. Francesconi, Curr. Opin. Solid State Mater. Sci. 3 (1998) 132–136.
[9] P.R. Slater, J. Fluor. Chem. 117 (2002) 43–45.
[10] E.E. McCabe, C. Greaves, J. Fluor. Chem. 128 (2007) 448–458.
[11] O. Clemens, P.R. Slater, Rev. Inorg. Chem. 33 (2013) 105–117.
[12] I.O. Troyanchuk, N.V. Kasper, O.S. Mantytskaya, E.F. Shapovalova, Mater. Res. Bull. 30 (1995) 421–425.
[13] Y. Inaguma, J.-M. Greneche, M.-P. Crosnier-Lopez, T. Katsumata, Y. Calage, J.-L. Fourquet, Chem. Mater. 17 (2005) 1386–1390.
[14] T. Katsumata, A. Takase, M. Yoshida, Y. Inaguma, J.E. Greedan, J. Barbier, L.M. D. Cranswick, M. Bieringer, Mater. Res. Soc. Symp. Proc. 988 (2007) 124–129.
[15] R. Heap, P.R. Slater, F.J. Berry, Ö. Helgason, A.J. Wright, Solid State Commun. 141 (2007) 467–470.
[16] F.J. Berry, F.C. Coomer, C. Hancock, Ö. Helgason, E.A. Moore, P.R. Slater, A.J. Wright, M.F. Thomas, J. Solid State Chem. 184 (2011) 1361–1366.
[17] F.J. Berry, R. Heap, Ö. Helgason, E.A. Moore, S. Shim, P.R. Slater, M.F. Thomas, J. Phys.:Condens. Matter 20 (2008) 215207/1–215207/6.
[18] C.K. Blakely, J.D. Davis, S.R. Bruno, S.K. Kraemer, M. Zhu, X. Ke, W. Bi, E.E. Alp, V.V. Poltavets, J. Fluor. Chem. 159 (2014) 8–14.
[19] O. Clemens, F.J. Berry, A.J. Wright, K.S. Knight, J.M. Perez-Mato, J.M. Igartua, P.R. Slater, J. Solid State Chem. 206 (2013) 158–169.
[20] J. Carvajal-Rodríguez, Physica B 192 (1993) 55–69.
[21] I.D. Brown, D. Altermatt, Acta Crystallogr. B41 (1985) 244–247.
[22] N.E. Brese, M. O'Keeffe, Acta Crystallogr. B47 (1991) 192–197.
[23] M.F. Collins, Magnetic Critical Scattering, Oxford University Press, New York, Oxford (1989) 29.
[24] T. Moriya "*Weak Ferromagnetism*" in Magnetism Vol. 1, G.T. Rado and H. Suhl eds. Academic Press Inc., New York, London (1963) pp. 93.
[25] J.A. Mydosh, Spin Glasses. An Experimental Introduction, Taylor and Francis Ltd., London (1993) 67.